

Nonlinear characteristics of a cylindrical Cherenkov laser at millimeter wavelengths

A. Hirata,^{a)} Y. Yuse, and T. Shiozawa

Department of Communication Engineering, Osaka University, Suita, Osaka 565-0871, Japan

(Received 10 December 2001; accepted for publication 19 March 2002)

Nonlinear characteristics of a cylindrical Cherenkov laser, which is composed of a dielectric-loaded coaxial waveguide and a hollow relativistic electron beam, are investigated with the use of particle simulation. The results obtained in this paper are compared with those for parallel plate and rectangular models. Numerical results show that, in the cylindrical Cherenkov laser, the electromagnetic (EM) wave grows exponentially in the longitudinal direction and reaches saturation, as is the case with the parallel plate and rectangular models. However, the efficiency of energy transfer from the electron beam to the EM wave in the cylindrical model is not in good agreement with that for the parallel plate model, especially for the case of a small radius of the inner conductor. Thus, we propose a modified parallel plate model whose growth characteristics are the same as those for the cylindrical model. With the use of the corresponding modified parallel plate model, one can calculate growth characteristics for the cylindrical model at a particular frequency more easily. © 2002 American Institute of Physics. [DOI: 10.1063/1.1477283]

I. INTRODUCTION

Although results achieved in mastering and utilization of electromagnetic (EM) radiation are very impressive over practically all frequency ranges, there still exists what is called the *millimeter-submillimeter-wave gap*.¹ The Cherenkov laser is one of the most promising candidates to cover this gap. Thus a great deal of experimental^{2–5} and theoretical^{6–16} work has been done on the Cherenkov laser over the last few decades.

In most theoretical articles on the Cherenkov laser published so far, some assumptions, i.e., lower dimensional assumptions, fluid theory for electron beams (e-beams), and so forth, were adopted for the sake of simplicity. However, little attention has been paid to the validity of such simplifications in the analysis of the Cherenkov laser. In other words, it is desirable to investigate the nonlinear characteristics of the growing EM wave in more actual situations. Thus, we analyzed a three-dimensional model of the Cherenkov laser composed of a dielectric-loaded rectangular waveguide and a finite-width planar relativistic e-beam,^{14,15} with the aid of particle simulation.^{17,18} On the other hand, growth characteristics for various cylindrical models of the Cherenkov laser^{2,3,7,10,13,16} have been investigated mainly in the microwave frequency range. In most of these papers, a linear or quasilinear fluid theory is adopted for the e-beam, that is, the nonlinear characteristics of the e-beam are not strictly taken into account.

In this paper, we analyze a cylindrical Cherenkov laser at millimeter wavelengths with the use of particle simulation. In particular, the results obtained are compared with those for the parallel plate¹¹ and rectangular models.^{14,15} Furthermore, we propose a corresponding parallel plate model whose growth characteristics are the same as those for the

cylindrical model. In particle simulation, the interaction between each particle (electron) constituting the e-beam and the EM wave is analyzed with the use of finite-difference time-domain (FDTD) method,^{19,20} instead of approximating the e-beam as a fluid.

II. BASIC EQUATIONS

The geometry of the problem is shown in Fig. 1, together with the coordinate system. The cylindrical Cherenkov laser under consideration consists of a dielectric-loaded coaxial waveguide and a hollow relativistic electron beam. We assume that the e-beam is magnetically confined in the z direction by a sufficiently large magnetostatic field, with all physical quantities assumed to be uniform in the ϕ direction.

The basic equations for the analysis are the Maxwell equations and the relativistic equation of motion for the electron. For the case where the e-beam is magnetically confined in the z direction by a sufficiently large magnetostatic field, electrons constituting the e-beam can move only in the z direction. Then, the relativistic equation of motion for a superparticle for electrons at the position (r_i, z_i) and with the velocity v_{zi} is expressed as

$$\frac{d}{dt}(\gamma_i m_e v_{zi}) = q_e E_z(r_i, z_i, t) \quad (1)$$

with

$$v_{zi} = \frac{dz_i}{dt}, \quad \gamma_i = \frac{1}{\sqrt{1 - (v_{zi}/c)^2}}, \quad (2)$$

m_e and q_e denoting the rest mass and the charge of a superparticle, and c the speed of light in vacuum. In particle simulation, we introduce the concept of superparticles with large mass and charge, which are composed of a large number of actual particles.^{17,18} By following the motion of superparticles in an EM field, we can properly describe the collective

^{a)}Email address: hirata@comm.eng.osaka-u.ac.jp

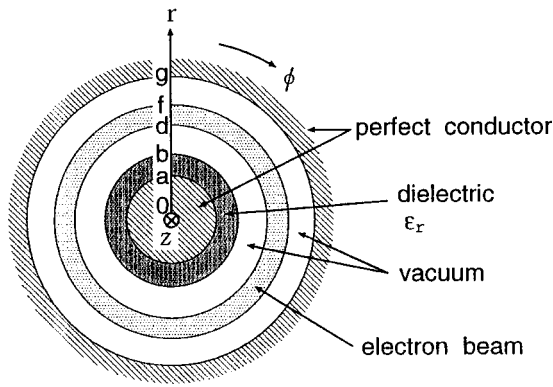


FIG. 1. Geometry of the problem.

behavior of individual particles in the field while greatly reducing the apparent number of particles involved and thus the time required for numerical simulation.

III. NUMERICAL ANALYSIS VIA PARTICLE SIMULATION

For numerical analysis of the interaction between an EM wave and the e-beam in the Cherenkov laser, we divide the cylindrical model for the Cherenkov laser shown in Fig. 1 into many small segments in the longitudinal direction, each of which is assumed to be one guide wavelength thick. Note that the guide wavelength is defined as the wavelength of the electromagnetic wave measured along a waveguide. We assume that the periodic boundary conditions are approximately satisfied between adjacent segments. Then, we pick out a group of particles contained in one particular segment at the initial state, and temporally follow the interaction between an EM wave and the particular group of particles as it travels down the waveguide. Each segment of the model for the Cherenkov laser is further subdivided into N_r subsegments in the r direction, and N_z subsegments in the z direction. The spatial grids subdividing a small segment in the r direction are spaced by Δr and numbered by j ($j = 0, 1, \dots, N_r$). Similarly, those in the z direction are spaced by Δz and numbered by k ($k = 0, 1, \dots, N_z$). We assume that the surfaces of the dielectric and the e-beam coincide with one of the spatial grids in the r direction. In the beam region of one particular segment, we arrange, at the initial state, two kinds of superparticles, one for electrons and the other for ions. Note that the number of particles involved in a superparticle is dependent on r , and represented by the following equation (see Fig. 2):

$$N(j) = n_0(j + 1/2)(\Delta r)^2 \Delta z \Delta \phi, \quad (3)$$

where we assume $\Delta \phi = 2\pi$ in our calculations. In addition, n_0 is the electron number density. Then, we follow the interaction between the superparticles for electrons and the EM wave while successively increasing time t from $t=0$ by an increment Δt , which must satisfy the following stability condition, what is known as a Courant condition, for numerical computation,

$$(c\Delta t)^2 \left[\frac{1}{(\Delta r)^2} + \frac{1}{(\Delta z)^2} \right] \leq 1. \quad (4)$$

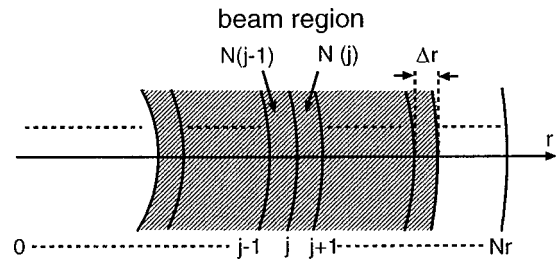


FIG. 2. Division of the model in the radial direction.

If we are given the initial conditions on the field distributions for an EM wave and on the positions and velocities for superparticles, we can follow step by step the interaction between an EM wave and a group of superparticles with the aid of the FDTD representations for basic equations described in Sec. II. In this paper, in order to simulate a single-pass Cherenkov oscillator, we give, at the initial state, a small sinusoidal velocity modulation on the e-beam, together with negligibly small field distributions.

IV. GROWTH CHARACTERISTICS OF A CYLINDRICAL CHERENKOV LASER

A set of various parameters used in this analysis is listed in Table I. The initial values for the velocity of superparticles and the frequency of the electromagnetic wave are chosen in such a way that the velocity matching between the electromagnetic wave of the lowest-order TM mode and the electron beam is satisfied. The frequency of the electromagnetic wave we picked out in the above manner is 124.0 GHz, which corresponds to the guide wavelength of 2.0 mm.

First, we discuss the energy transfer rate from the e-beam to the EM wave. We define the rate of energy transfer from the e-beam to the EM wave at $t = n\Delta t$ (Δt = time increment, $n = 0, 1, 2, \dots$), $\eta(n)$, as the rate of energy transfer from the kinetic energy carried by the e-beam to the EM wave energy, i.e., as

$$\eta(n) = \frac{W_{em}^n}{W_p^0} = \frac{W_p^n - W_p^0}{W_p^0}, \quad (5)$$

where W_{em}^n and W_p^n denote the EM wave energy and the beam kinetic energy at $t = n\Delta t$, respectively, and W_p^0 the initial value of the beam kinetic energy.

TABLE I. Values of various parameters used for the numerical simulation.

Guide wavelength λ_g	2.0 (mm)
Thickness of dielectric sheet $\tau(b-a)$	0.5 (mm)
Beam-dielectric gap $(d-b)$	0.5 (mm)
Beam thickness $(f-d)$	0.125 (mm)
Radius of inner conductor a	3.0 (mm)
Separation between outer and inner conductors $(g-a)$	2.0 (mm)
Relative permittivity ϵ_r	2.12
Initial beam velocity v_0/c	0.813
Frequency of EM wave $\omega/2\pi$	124.0 (GHz)
Plasma frequency for electrons $\omega_p/2\pi$	0.954 (GHz)
Electron number density n_0	2.01×10^{10} (/cm ³)

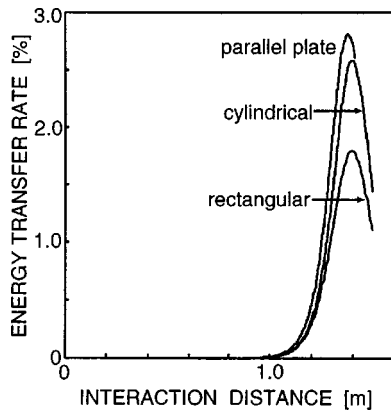


FIG. 3. Spatial variation of energy transfer rate.

We show in Fig. 3 the spatial variation of the energy transfer rate from the e-beam to the EM wave. Note that in Fig. 3 the interaction distance denotes the distance that a group of superparticles has traveled with their average velocity during the interaction time t . For comparison, we also show those for the parallel plate¹¹ and rectangular models.¹⁴ As seen from Fig. 3, the energy transfer rate for each model grows exponentially in the longitudinal direction and reaches saturation around $z=1.40$ m. Additionally, the maximum value of the energy transfer rate, which corresponds to the efficiency of energy transfer from the electron beam to the EM wave, for the cylindrical model is slightly less than that for the parallel plate model, although the electric field acts on the e-beam uniformly for the former case. In order to explain why this is the case, we show in Fig. 4 the dispersion curve for both the parallel plate and cylindrical models. We should notice that the dispersion relations for the EM wave modes for the parallel plate and cylindrical models are given in the following equations: for the parallel plate waveguide model,

$$\frac{p_r}{\epsilon_r} \tan(p_r(b-a)) - h_r \tanh(h_r(g-b)) = 0, \quad (6)$$

and for the cylindrical model,

$$\frac{p_r J_0(p_r a) N_0(p_r b) - J_0(p_r b) N_0(p_r a)}{\epsilon_r J_0(p_r a) N_1(p_r b) - J_1(p_r b) N_0(p_r a)} - h_r \frac{I_0(h_r b) K_0(h_r g) - I_0(h_r g) K_0(h_r b)}{I_1(h_r b) K_0(h_r g) - I_0(h_r g) K_1(h_r b)} = 0, \quad (7)$$

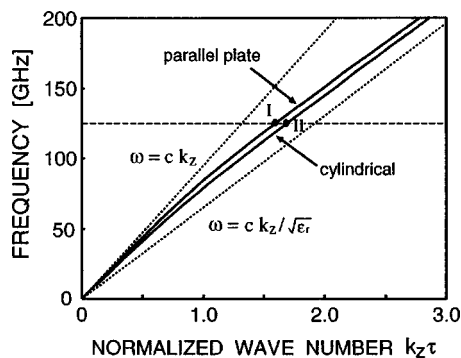


FIG. 4. Dispersion curves for EM wave modes.

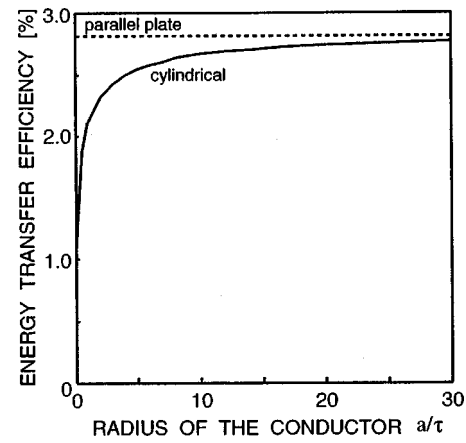


FIG. 5. Dependence of energy transfer efficiency on the radius of the inner conductor.

where

$$p_r = \sqrt{\epsilon_r (\omega/c)^2 - k_z^2},$$

$$h_r = \sqrt{k_z^2 - (\omega/c)^2}.$$

Note that we consider, respectively, the TM_1 mode for the parallel plate model and the TM_{01} mode for the cylindrical model, which are the dominant modes interacting with the e-beam. In addition, J_n , N_n , I_n , and K_n ($n=0,1$) are, respectively, the Bessel functions of the first and second kinds, and the modified Bessel functions of the first and second kinds. As seen from Fig. 4, at the same frequency, the longitudinal wave number for the parallel plate model is slightly smaller than that for the cylindrical model, leading to a larger value of h_r for the latter model. Therefore, the EM fields for the latter model concentrate more on the dielectric sheet, resulting in a weaker beam-wave coupling. On the other hand, the reason why the energy transfer efficiency for the rectangular model is the smallest of all is that the electric field acting on the e-beam is nonuniform in the x direction for this model, as mentioned in Ref. 14.

Next, we show in Fig. 5 the dependence of the energy transfer efficiency on the radius of the inner conductor a . The difference in energy transfer efficiency between the cylindrical and parallel plate models is significant, especially for smaller values of a . In other words, we can reasonably approximate growth characteristics of the cylindrical model with those of the parallel plate model for larger values of a . On the other hand, the difference in energy transfer efficiency between two models becomes significant with decreasing a . The reason for this is that more EM energy is concentrated around the dielectric sheet for the cylindrical model as a becomes smaller.

V. PROPOSAL OF AN EQUIVALENT PARALLEL PLATE MODEL

In the last section, we showed that the characteristics for the cylindrical model deviate significantly from those for the parallel plate waveguide model as the radius of an inner conducting cylinder a decreases. However, as will be seen, we can estimate the growth characteristics for the cylindrical

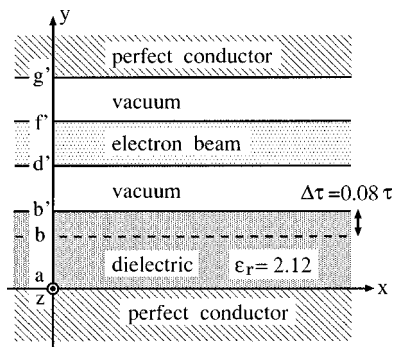


FIG. 6. Equivalent parallel plate model for the cylindrical model with the parameter of $a/\tau = 6$. $p' = p + \Delta\tau$ ($p = b, d, f$, and g).

model more easily by replacing it by an equivalent parallel plate model. By defining an equivalent parallel plate model, we can avoid some complexities encountered in the numerical treatment of the cylindrical model, such as the dependence of the number of actual particles involved in a superparticle on radius r , the weighting of a particle on FDTD grids, and so forth. On the other hand, we observed in the last section that the significant difference in energy transfer efficiency between two models is due to the difference in the intensity of the electric field acting on the e-beam. Thus, the difference in energy transfer efficiency between two models would be suppressed if the intensity of the electric field acting on the e-beam for the parallel plate model could be made equal to that for the cylindrical model. For this purpose, we propose to vary the dielectric thickness $\tau (= b - a)$ so that the wave number for the parallel plate model coincides with that for the cylindrical model (see the points I and II in Fig. 4). Note that the values of the other parameters are kept the same as shown in Table I. Specifically, the above-mentioned condition is satisfied with the increase in the dielectric thickness by 8 % for $a/\tau = 6$ (see Fig. 6).

In order to demonstrate the validity of our scheme, we show in Fig. 7 the relative difference of energy transfer efficiency between the cylindrical model, and the conventional and equivalent parallel plate approximations. As seen from Fig. 7, the relative difference of the improved parallel plate model is dramatically suppressed as compared with that for the conventional parallel plate approximation. Thus, with the use of the corresponding modified parallel plate model, we can calculate the growth characteristics of the cylindrical model more easily.

VI. CONCLUSION

In this paper, the nonlinear characteristics of a cylindrical Cherenkov laser, which consists of a dielectric-loaded coaxial waveguide and a hollow relativistic electron beam, were investigated with the use of the FDTD method incorporated with particle simulation. The results obtained were compared with those for the parallel plate and rectangular models. Numerical results showed that in the cylindrical Cherenkov laser the EM wave grows exponentially in the longitudinal direction and reaches saturation, as is the case with the parallel plate and rectangular models. The energy

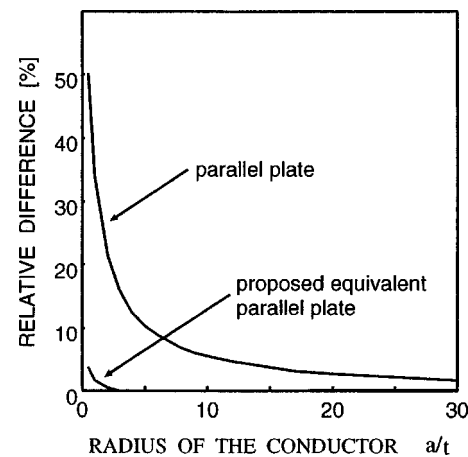


FIG. 7. Relative difference of energy transfer efficiency between the cylindrical model and the 2D models.

transfer rate from the e-beam to the EM wave for the cylindrical model is in good agreement with that for the parallel plate model only for the case of a large radius of the inner conducting cylinder. On the other hand, it decreases for a smaller radius of the inner conductor. Then, we proposed to vary the dielectric thickness with the aid of dispersion diagram so that the wave number in the z direction for the parallel plate model coincides with that for the cylindrical model at a particular frequency. The validity of our scheme was confirmed by numerical examples. Thus, one can calculate more easily the growth characteristics of the cylindrical model at a particular frequency with the use of a corresponding equivalent parallel plate model. By using an equivalent parallel plate model, one can avoid some complexities encountered in the cylindrical model.

- ¹A. V. Gaponov-Grekhov and V. L. Granatstein, *Applications of High-Power Microwave* (Artech House, Norwood, 1994).
- ²J. E. Walsh, T. C. Marchall, and S. P. Schlesinger, *Phys. Fluids* **20**, 709 (1977).
- ³K. L. Felch, K. O. Busby, R. W. Layman, D. Kapilow, and J. E. Walsh, *Appl. Phys. Lett.* **38**, 601 (1981).
- ⁴E. P. Garate, J. E. Walsh, C. Shaughnessy, B. Johnson, and S. Moustazis, *Nucl. Instrum. Methods Phys. Res. A* **259**, 125 (1987).
- ⁵F. Ciocci, A. Doria, G. P. Gallerano, I. Giabba, M. F. Kimmitt, G. Messina, A. Renieri, and J. E. Walsh, *Phys. Rev. Lett.* **66**, 699 (1991).
- ⁶J. E. Walsh and J. B. Murphy, *IEEE J. Quantum Electron.* **18**, 1259 (1982).
- ⁷M. Shoucri, *Phys. Fluids* **26**, 2271 (1983).
- ⁸V. K. Tripathi, *J. Appl. Phys.* **56**, 1953 (1984).
- ⁹T. Shiozawa and H. Kondo, *IEEE J. Quantum Electron.* **23**, 1633 (1987).
- ¹⁰K. Horinouchi, I. Hirakawa, and T. Shiozawa, *IEICE Trans.* **J75-C-I**, 188 (1992) (in Japanese).
- ¹¹K. Horinouchi, M. Sanda, H. Takahashi, and T. Shiozawa, *IEICE Trans.* **J78-C-I**, 1 (1995).
- ¹²T. Shiozawa and T. Yoshitake, *IEEE J. Quantum Electron.* **31**, 539 (1995).
- ¹³P. Mardahl, J. P. Verboncoeur, and C. K. Birdsall, *IEEE International Conference on Plasma Science*, Boston, 1996, p. 256.
- ¹⁴A. Hirata and T. Shiozawa, *IEEE J. Quantum Electron.* **34**, 1802 (1998).
- ¹⁵A. Hirata and T. Shiozawa, *J. Appl. Phys.* **82**, 5907 (1997).
- ¹⁶Y. Seo, E. H. Choi, and G. S. Cho, *J. Phys. D* **33**, 654 (2000).
- ¹⁷R. W. Hockney and J. W. Eastwood, *Computer Simulation Using Particles* (McGraw-Hill, New York, 1981).
- ¹⁸C. K. Birdsall and A. B. Langdon, *Plasma Physics via Computer Simulation* (McGraw-Hill, New York, 1985).
- ¹⁹K. S. Yee, *IEEE Trans. Antennas Propag.* **14**, 302 (1966).
- ²⁰A. Taflov, *Computational Electrodynamics: The Finite-Difference Time-Domain Method* (Artech House, Norwood, 1995).